Differentially Private Graph Neural Networks for Link Prediction

Xun Ran†, Qingqing Ye†*, Haibo Hu†, Xin Huang‡, Jianliang Xu‡, Jie Fu†
†The Hong Kong Polytechnic University, ‡Hong Kong Baptist University
qi-xun.ran@connect.polyu.hk *qqing.ye@polyu.edu.hk* *haibo.hu@polyu.edu.hk*
xinhuang@comp.hkbu.edu.hk *xujl@comp.hkbu.edu.hk* *jie.fu@stu.ecnu.edu.cn*

***Abstract*—Graph Neural Networks (GNNs) have proven to be highly effective in addressing the link prediction problem. However, the need for large amounts of user data to learn representations of user interactions raises concerns about data privacy. While differential privacy (DP) techniques have been widely used for node-level tasks in graphs, incorporating DP into GNNs for link prediction is challenging due to data dependency. To this end, in this work we propose a differentially private link prediction (DPLP) framework, building upon subgraph-based GNNs. DPLP includes a DP-compliant subgraph extraction module as its core component. We first propose a neighborhood subgraph extraction method, and carefully analyze its data dependency level. To reduce this dependency, we optimize DPLP by integrating a novel path subgraph extraction method, which alleviates the utility loss in GNNs by reducing the noise sensitivity. Theoretical analysis demonstrates that our approaches achieve a good balance between privacy protection and prediction accuracy, even when using GNNs with few layers. We extensively evaluate our approaches on benchmark datasets and show that they can learn accurate privacy-preserving GNNs and outperforms the existing methods for link prediction.**

***Index Terms*—Data privacy, Link prediction, Graph neural networks, Differential privacy**

I. Introduction

Link prediction is the problem of predicting the existence of a link between two nodes within a graph [1]. Given the ubiquitous existence of graph data, this field finds applications in a multitude of domains, such as friend recommendation within social networks [2], movie recommendation on Netflix [3], co-authorship prediction in citation networks [4]. Recently, graph neural networks (GNNs) have shown superior performance in link prediction when compared to traditional methods [5], [6]. In particular, by leveraging a localized subgraph surrounding each target link, subgraph-based GNNs (SGNNs) have been demonstrated to learn the most expressive structural representations of links for prediction.

On the other side of the coin of using GNN models for link prediction, the users' privacy is at risk. Privacy breaches can happen in various ways since an attacker can infer sensitive node features or links from the trained models [7], [8]. Differential Privacy (DP) has received significant attention in incorporating it into GNN-based methods to mitigate the privacy risks. However, current studies primarily focus on developing differentially private GNNs for node classification [9]–[13], leaving a noticeable gap in research concerning link prediction. To bridge the gap, our work focuses on learning GNNs for accurate link prediction while preserving differential privacy.

Extending approaches designed for node-level tasks to link prediction is nontrivial. In GNNs, learning the representation of each node relies not only on its own features but also on aggregated information from its neighborhood. This introduces a complex data dependency issue, which poses additional challenges in the context of link prediction compared to node-level tasks. To illustrate the challenges, Figure 1 shows an example involving a 1-hop neighborhood subgraph.

Example 1. *In node-level tasks, to determine the nodes affected when a specific node s is removed, we can simply count its 1-hop neighbors (i.e., nodes a, b, c, d in Figure 1 (a)). The number of affected nodes is bounded by the maximum node degree θ, which is 4 in this case. Regarding link prediction, removing the link (s, q) in Figure 1 (b) will affect all the red links since they all have their 1-hop neighborhood subgraphs containing the link (s, q). However, enumerating these affected links becomes challenging because their relative positions to (s, q) vary from case to case (e.g., links $(q, b), (q, a), (c, d)$). Additionally, to train a link prediction model, we should also consider the non-existent links (e.g., (a, b)) sampled as negative examples. In the worst case, the total number of affected links can reach $\Omega(\theta^2)$.*

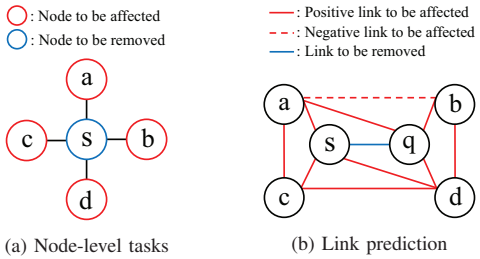

(a) Node-level tasks (b) Link prediction

Fig. 1: Data dependency issues in 1-hop subgraph, with the maximum node degree $\theta = 4$.

Accurately measuring data dependency is crucial for calculating noise sensitivity to comply with DP. In the literature, two paradigms have been studied to address the issue of data dependency in GNNs. **The first approach is to avoid the complexity of measuring dependencies** by introducing DP noise to either the input, such as adjacency matrix [9], or the aggregation functions [10] used in GNNs. However, the

* Corresponding author.

2375-026X/24/$31.00 ©2024 IEEE
DOI 10.1109/ICDE60146.2024.00133

former often introduces excessive noise that compromises the model utility, and the later lacks adaptability to diverse GNN architectures since the aggregation function is non-learnable. Moreover, this approach suffers from a loss of model utility as the depth of GNNs increases.

The second paradigm measures the dependency among nodes, focusing on the task of node classification [13]. In particular, an upper bound of interdependent nodes is derived by sampling the incoming neighbors of any nodes in a graph. However, this approach cannot be directly applied to link prediction for several reasons: (i) The dependency analysis of node-level tasks considers neighboring nodes, but there is no off-the-shelf definition of neighboring links. (ii) Link prediction requires considering the neighborhoods of both two nodes, introducing a higher level of dependency compared to node classification. (iii) To train a link prediction model, it is essential to account for non-existent links (e.g., link (a, b) in Figure 1(b)), as their presence increases the noise sensitivity. These factors collectively contribute to the increased complexity of dependency analysis for link prediction.

In this work, we propose a differentially private link prediction (DPLP) framework based on GNNs, which is compatible with various GNN blocks with learnable aggregation functions. In the framework, the sensitivity analysis module introduces the notion of link-based subgraph contextual neighbor and gives the theoretical results of dependency level. To constrain the dependency level, our framework employs a graph projection step to bound the node degree and a subgraph extraction step with a tunable negative sampling rate. Our method yields a tight upper bound of dependency level for determining a sound noise scale to comply with DP.

To improve the utility, we propose an optimized path-based subgraph extraction module for the DPLP framework. This method is built upon the observation that the prevailing subgraph extraction technique often generates subgraphs containing dangling edges. Such dangling edges amplify inter-subgraph dependencies but offer limited contribution to link prediction. By dropping these edges, the information carried by the subgraph is confined to the paths connecting the nodes of a target link. Consequently, this reduces the dependency level while preserving link structural information. As a result, this optimization leads to higher prediction accuracy while maintaining strict privacy requirements. Overall, the contributions of our work are summarized as follows:

- We propose a differential privacy-preserving link prediction (DPLP) framework. To the best of our knowledge, this is the first framework to learn differentially private GNN for link prediction. This framework is adaptable to various GNN architectures.
- We design an optimized path-based subgraph extraction module for the DPLP framework, which reduces data dependency by focusing on the paths connecting the nodes of a target link, resulting in improved prediction accuracy.
- We conduct extensive theoretical analysis on both privacy and utility aspects. In particular, we prove that our algorithm approximates the predictive performance of multi-layer GNNs using fewer layers.
- We evaluate the effectiveness of DPLP over real-world datasets. The experimental results validate our theoretical findings and demonstrate the effectiveness of the proposed methods. The results also present that our method strikes a balance between link prediction accuracy and privacy protection.

The remainder of this paper is organized as follows. Section II reviews related works. Section III introduces preliminaries and the studied problem. Section IV presents the overview and the implementation details of the DPLP framework. Section V proposes the optimized path-based subgraph extraction method. Section VI shows the theoretical analysis of the proposed methods. Section VII presents the experimental results, followed by a conclusion in Section VIII.

II. Related Work

Traditional link prediction techniques include heuristic, latent-feature, and content-based methods. Heuristic methods like Common Neighbors and Adamic-Adar [1], [2] estimate link probabilities based on node similarity. Latent-feature methods learn node embeddings through matrix factorization, exemplified by DeepWalk and node2vec [14], [15]. Content-based methods, on the other hand, utilize node attributes [16].

Recent advancements in link prediction are led by Graph neural networks (GNNs), which outshine traditional methods by integrating graph structure with node/edge features. Among GNN-based approaches, subgraph-based methods have emerged as particularly effective [6], [17]. These methods focus on local subgraphs around target links, applying a GNN to learn representations for each subgraph, which then serve as link representations for prediction.

Zhang et al.'s analysis [5] reveals that subgraph-based methods excel over node-based methods in link prediction by effectively capturing the relational context within local subgraphs. While node-based methods falter in recognizing the relative positioning of node pairs due to their isolated learning approach, subgraph-based methods overcome this limitation without deep GNNs. The impracticality of deep GNNs in privacy-sensitive environments, owing to escalating data dependencies, further underscores the suitability of subgraph-based approaches, as a foundational framework for privacy-preserving link prediction.

Research in link prediction privacy is bifurcated into centralized and decentralized approaches. Decentralized scenarios involve collaboration among entities holding different parts of graph data, aiming to secure data transactions and prevent privacy breaches [9], [18]. Centralized models, conversely, focus on developing robust privacy-preserving models to resist attacks like model inversion and membership inference [7], [8], [19]. Significantly, research has shown that link existence alone can disclose sensitive user information [20], [21], underscoring the importance of link-level privacy in centralized settings. This work considers the problem of link prediction preserving link-level privacy in a centralized setting.

Differential Privacy (DP) has been extensively applied to link prediction methods, including heuristic and latent-feature approaches [22]–[26]. Traditional DP applications, such as DP-SGD [27], face challenges with GNNs due to data dependency issues, where computations rely on interconnected user data, increasing privacy risks.

To address this, DP in GNNs is approached through input perturbation, aggregation function perturbation, and gradient perturbation [9], [10], [12], [13]. Input perturbation adds noise to the graph data, aggregation function perturbation modifies GNN's message passing, and gradient perturbation involves noise addition in GNN gradients. While each technique manages data dependencies, they also face limitations like signal loss or reduced learnability.

Mueller et al. proposed a DP method for graph-level tasks [28], and Peng et al. proposed a differentially private method for learning graph embeddings of federated knowledge graphs [29]. However, the two methods are under the assumption of independent instances in the training set, a condition not always met in link prediction. Considering these limitations, this work aims to develop an algorithm that ensures DP while maintaining a balance between utility and privacy, and is adaptable across various GNN modules.

III. Preliminaries and Problem Formulation

A. Notations

Let $G = (V, E)$ be an undirected graph where V is the set of nodes, E is the set of observed links, and $d(u, v)$ denotes the shortest path between a pair of nodes u and v. For a node u, its h-hop neighbors is denoted as $N_h(u) = \{v \mid d(u, v) = h, v \in V\}$, and its h-hop neighborhood is $\Gamma_h(u) = \cup_{i=0}^{h} N_i(u)$. Noted that nodes in $N_h(u)$ are exactly h hops away from u, and $N_0(u)$ denotes the node u itself.

Let $S = (V_S \subseteq V, E_S \subseteq E)$ be a subgraph of G, it can be extracted by a function $g : G \times \mathcal{E} \times \mathbb{N} \to S$. Here, $\mathcal{E}$ is an entity set, the elements of which can be either a vertex $u \in V$ or a pair of vertices $u, v \in V$. Any positive integer $h \in \mathbb{N}$ denotes the size of the extracted subgraph. Let $z \in \mathcal{E}$, S_z represents the enclosing subgraph that captures the local structure around z.

In addition to the concepts mentioned above, the main notations within this paper are listed in Table I.

TABLE I: Notations

Notation	Description
G	Undirected graph
V	Node set
E	Edge set
$\mathbf{A}$	Adjacency matrix
$\mathbf{X}$	Node feature matrix
$\mathcal{E}$	Entity set of a vertex or a pair of vertices.
S_z	Enclosing subgraph of z, where $z \in \mathcal{E}$.
$d(u, v)$	Shortest distance between u and v
$N_h(u)$	Node u's h-hop neighbors: $\{v \mid d(u, v) = h, v \in V\}$
$\Gamma_h(u)$	H-hop neighborhood of node u: $\cup_{i=0}^{h} N_i(u)$
$\Gamma_h(u, v)$	H-hop neighborhood of link (u, v): $\Gamma_h(u) \cup \Gamma_h(v)$
$LSN_h^g(s, q)$	Set of link-based subgraph contextual neighbors of (s, q)

B. Graph Neural Networks

Let $G = (V, E)$ be an undirected graph with an adjacency matrix $\mathbf{A} \in \{0, 1\}^{n \times n}$, where $n = |V|$. An r-layer GNN is a parametric function that can be represented by the following node-wise operations:

$$\begin{aligned} \mathbf{h}_u &= \mathrm{GNN}(\mathbf{A}, \mathbf{x}_u, \mathbf{\Theta}) \\ &= \psi\left(\mathbf{x}_u, \omega\left(\{\phi(\mathbf{x}_u, \mathbf{x}_v) \mid v \in \Gamma_r(u)\}\right)\right) \end{aligned} \tag{1}$$

where $\mathbf{x}_u \in \mathbb{R}^d$ and $\mathbf{h}_u \in \mathbb{R}^{d'}$ are d-dimensional input and d'-dimensional output features of node u, respectively. All functions ψ, ω, ϕ are learnable, and the parameters of the whole network are denoted as $\mathbf{\Theta}$. The above equation can be written in matrix representation as $\mathbf{H} = \mathrm{GNN}(\mathbf{A}, \mathbf{X}, \mathbf{\Theta})$ across all nodes, where $\mathbf{X} \in \mathbb{R}^{n \times d}$ is the node features, and $\mathbf{H} \in \mathbb{R}^{n \times d'}$ is the node representations.

C. Subgraph-based GNNs (SGNNs)

Given an undirected graph $G = (V, E)$ and a target $z \in \mathcal{E}$ (i.e., one or two nodes), SGNNs produce the embeddings $\mathbf{H}_z = \mathrm{GNN}(\mathbf{A}_z, \mathbf{X}_z, \mathbf{\Theta})$, where $\mathbf{A}_z$ presents the structure of the enclosing subgraph S_z, and $\mathbf{X}_z$ are the features of the nodes in S_z. Capturing the local structure, the embeddings can be effective for the downstream tasks.

In particular, for link prediction, the most common definition of the enclosing subgraph is the h-hop neighborhood subgraph. Its formal definition is as follows:

Definition 1 (H-Hop Neighborhood Subgraph)**.** *Given an undirected graph $G = (V, E)$ and a pair of distinct nodes $u, v \in V$, (u, v)'s h-hop neighborhood subgraph S_{uv} is the subgraph induced by the union of u's and v's h-hop neighborhood $\Gamma_h(u, v) = \Gamma_h(u) \cup \Gamma_h(v)$, i.e., $S_{uv} = g_n(G, (u, v), h)$, where g_n is the subgraph extraction function specific to the context of neighborhood.*

SGNNs can approximate global heuristics (i.e., graph structural features) from the h-hop neighborhood subgraph. The precision loss of this approximation diminishes exponentially with h [6].

D. Link-level Differential Privacy

This study aims to protect private links by applying differential privacy. As with the existing work [9], [30], we first define neighboring graphs and link differential privacy as follows.

Definition 2 (Neighboring Graphs)**.** *Two graphs G and G' are neighboring graphs if one can be obtained by adding or removing a link to the other.*

Definition 3 (Link Differential Privacy)**.** *A randomized mechanism $\mathcal{M}$ satisfies (ε, δ)-link differential privacy, if and only if for any two neighboring graphs G, G', and any possible output $\mathcal{Z} \subseteq range(\mathcal{M})$, the following inequality holds:*

$$Pr(\mathcal{M}(G) \in \mathcal{Z}) \leq \varepsilon \cdot Pr(\mathcal{M}(G') \in \mathcal{Z}) + \delta.$$

Intuitively, a randomized algorithm $\mathcal{M}$ is said to be link-level differentially private if the addition or removal of a link in

$\mathcal{M}$'s input does not affect $\mathcal{M}$'s output significantly. As shown below, the impact of the link difference between neighboring graphs influences the sensitivity analysis, which is critical to determine the noise scale in compliance with DP.

Definition 4 (Sensitivity under link differential privacy)**.** *The sensitivity $\Delta(f)$ of a function f defined on graph datasets is*

$$\Delta(f) = \max_{G,G'} \|f(G) - f(G')\|.$$

E. Problem Formulation

This work studies the problem of link prediction, which aims to predict the probability, denoted as $p(u, v)$, of a link between two nodes u and v. In this context, SGNNs have demonstrated effectiveness, and the link probability is computed based on the enclosing subgraph S_{uv}. Formally,

$$p(u, v) = R(\text{GNN}(\mathbf{A}_{uv}, \mathbf{X}_{uv}, \mathbf{\Theta})), \tag{2}$$

where R is a learnable readout function.

Our work focuses on the problem of designing an algorithm to learn GNNs while preserving link differential privacy. The difficulty in sensitivity analysis makes this problem non-trivial. Due to the data dependency issue in GNNs, the sensitivity requires a careful analysis of the maximum number of link embeddings that are affected by the removal of a link. This requires us to develop an analytical approach to derive a tight upper bound of this quantity to constrain the dependency level.

IV. Differentially Private Link Prediction

In this section, we propose a GNN-enabled framework for differentially private link prediction (DPLP). We first show an overview of the framework DPLP in Section IV-A, and then elaborate on the implementation details in Section IV-B.

A. DPLP Overview

DPLP framework is designed to train a link prediction model that is compatible with a wide range of GNN architectures, balancing differential privacy (DP) protection and model utility. DPLP works as shown in Figure 2, which includes three modules, namely subgraph extraction, sensitivity analysis, and DPGNN training. In what follows, we will present the design rationale of each module.

Subgraph Extraction. Following the success of SGNNs in capturing the local structure, DPLP incorporates SGNNs for link embedding and integrates a subgraph extraction module to support different subgraph extraction functions. Before subgraph extraction, DPLP includes a graph-specific projection step. This is because, the scale of DP noise increases exponentially with the maximum node degree, as will be elaborated in Lemma 3. To address the issue, this step projects the original graph to ensure a maximum node degree θ. In conjunction with the negative sampling in subgraph extraction, this step efficiently reduces and bounds the noise scale.

Sensitivity Analysis. We incorporate a sensitivity analysis module to examine link dependency by introducing the concept of link-based subgraph contextual neighbor, ensuring a precise and optimized sensitivity measure for link differential privacy.

DPGNN Training. Gradient perturbation is a paradigm solution for training differentially private GNN. Due to its architecture-agnostic nature, the paradigm allows the private learning to be applied across different GNNs and aggregation functions. However, conventional gradient perturbation methods, such as DP-SGD [27], are not directly applicable to GNNs. This arises from the inherent structure of GNNs where each per-sample (or per-link) gradient is influenced by private links from multiple users. This complexity poses challenges in determining an appropriate noise scale for achieving private gradients. In DPLP, this interdependency measured by the sensitivity analysis module allows us to accurately control the noise magnitude to derive the private gradient. Additionally, in Section VI, we will demonstrate that our perturbation approach also amplifies privacy.

Putting three modules together leads to our framework DPLP. As shown in Figure 2, the original graph $G = (V, E)$ is projected to graph G^θ with a maximum node degree θ (step (1)). For every edge in the projected graph G^θ, including those from negative sampling, their respective subgraphs are extracted. These subgraphs, paired with their labels, form the training dataset (step (2)). Given the subgraph extraction function g, and the subgraph size h, the maximum number of subgraph contextual neighbors of any link in G is computed, i.e., $\max_{(s,q)\in E} |LSN_h^g(s, q)|$ (step (3)). Then, the sensitivity is derived (step (4)). The progression of training the differentially private GNN is presented in steps (5) - (9). Initially, a batch of subgraphs is uniformly sampled from the training set and fed into the GNN (step (5)). The gradient perturbation mechanism involves two steps, namely clipping per-sample gradients (step (6)) and injecting noise into the batched gradient to yield a private gradient vector (step (8)), where the noise is sampled according to the sensitivity (step (7)). This sequence, spanning from step (5) to step (9), is iterated until the stop condition is achieved. Finally, DPLP outputs a trained GNN model preserving link differential privacy.

B. DPLP Implementation

In this section, we shows the implementation details of DPLP. In particular, we first present subgraph extraction and DPGNN training, followed by sensitivity analysis which introduces the notion of link-based subgraph contextual neighbor and gives the theoretical results.

1) Subgraphs Extraction: Given a maximum node degree of θ, the graph projection step projects the original graph into G^θ so that the degree of each node is bounded by θ. As outlined in Algorithm 1 (Lines 9-15), for each node v, we randomly sample at most θ immediate neighbors from E^θ of G^θ, and update the edges in E^θ by dropping the edges between v and the excessive neighbors. The parameter θ decides the number of available samples for the training module and the scale of influence when a link is removed, which in turn affects

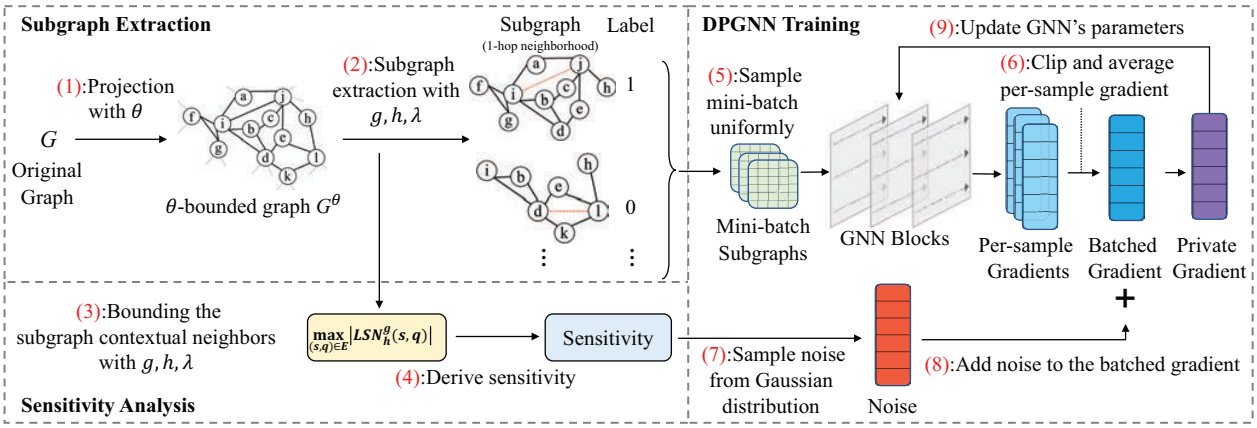

Fig. 2: The overview of the DPLP framework.

the sensitivity of DP noise. In Section 5.2, we will delve into the selection of this parameter.

Then the subgraph extraction step extracts a set of subgraphs along with their node labels, constituting training dataset for link prediction model. The purpose is to acquire the local structure of the target link to be classified. Specifically, for each link in projected graph G^θ, we will extract a corresponding subgraph, which serves as a positive sample in the training dataset. To prevent model bias, we sample some non-existent links and extract their subgraphs as negative samples.

Algorithm 1 demonstrates the neighborhood subgraph extraction process. Note that for each node v, there are $|N_1(v)|$ positive links. Thus, given the negative sampling rate λ, $\lambda|N_1(v)|$ negative links will be sampled from $V \backslash N_1(v)$ (Line 3). Then for each positive or negative link, a subgraph will be extracted by the subgraph extraction function g_n (Line 6), along with a binary label (Line 7).

2) Training Differentially private GNNs: Learning a GNN is equivalent to finding optimal parameters $\mathbf{\Theta}^*$ that minimizes the loss function $\mathcal{L}(\mathcal{S}, \mathbf{\Theta})$. Formally

$$\begin{aligned}\mathbf{\Theta}^* &= \arg\min_{\mathbf{\Theta}} \mathcal{L}(\mathcal{S}, \mathbf{\Theta}) \\ &= \arg\min_{\mathbf{\Theta}} \sum_{S_{uv}, y_{uv} \in \mathcal{S}} \ell\left(R\left(\text{GNN}\left(\mathbf{A}_{uv}, \mathbf{X}_{uv}, \mathbf{\Theta}\right)\right), y_{uv}\right),\end{aligned} \tag{3}$$

where $\mathcal{S}$ is the training subgraphs returned by Algorithm 1. The learning algorithm towards the above loss is summarized in Algorithm 2. First, the training set is established (Line 1), and the noise scale σ is computed via sensitivity analysis (Line 2). Next, we iteratively update the GNN model after model initialization. In iteration t, a batch $\mathcal{B}_t$ of m subgraphs is uniformly sampled from $\mathcal{S}$. It guarantees each subgraph appears only one time within $\mathcal{B}_t$. Subsequently, per-sample gradients are computed and clipped (Lines 7-10) with a given l^2 norm threshold C. Gaussian noise is added to the batched gradient that is aggregated from clipped per-sample gradients (Lines 11-12). The private gradients are employed for model updating. This process continues until the maximum number of iterations T is reached.

Algorithm 1: EXTRACT-SUBGRAPHS (Extract Neighborhood Subgraphs)

Data: Graph $G = (V, E)$; Maximum node degree θ;
Negative sampling rate λ; Neighborhood radius h;
Neighborhood subgraph extraction function g_n.
Result: Set of subgraphs S_{uv} and lables y_{uv} for target links.

1 $G^\theta \leftarrow \text{PROJECTION}(G, \theta), NE \leftarrow \emptyset$.
2 **for** $v \in V$ **do**
3 Uniformly sample negative edges of v with λ: $\bar{N}_1(v) \leftarrow \text{sample}(V \backslash N_1(v), \lambda|N_1(v)|)$.
4 Add the negative edges to NE.
5 **for** $i \in N_1(v) \cup \bar{N}_1(v)$ **do**
6 Extract subgraph: $S_{vi} \leftarrow g_n(G^\theta, (v, i), h)$.
7 $y_{vi} = \begin{cases} 1 & \text{if } i \in N_1(v); \\ 0 & \text{otherwise.} \end{cases}$
8 **return** $\{S_{uv}, y_{uv} \mid (u, v) \in E^\theta \cup NE\}$.
9 **Function** PROJECTION(G, θ):
10 Initialize $G^\theta = (V, E^\theta) \leftarrow G$.
11 **for** $v \in V$ **do**
12 $N_1^\theta(v) \leftarrow$ Randomly sample at most θ immediate neighbors of v by E^θ.
13 $e = \{(u, v) \mid u \in \{N_1(v) \backslash N_1^\theta(v)\}\}$.
14 Update E^θ by dropping edges in e from E^θ.
15 **return** $G^\theta = (V, E^\theta)$.

3) Sensitivity Analysis: For sensitivity analysis in subgraph-based GNNs, understanding link dependency is crucial. While node-level tasks leverage neighboring relationships to measure node dependency, no such standard exists for links. Consequently, we introduce the notion of link-based subgraph contextual neighbor to describe the interdependency between links.

Definition 5 (Link-based Subgraph Contextual Neighbor)**.** *Given an undirected graph $G = (V, E)$, a pair of nodes $u, v \in V$, a subgraph extraction function g and the subgraph size h. If the subgraph $g(G, (u, v), h)$ contains a link (s, q), then (u, v) is a subgraph contextual neighbor of (s, q), which is denoted as $(u, v) \in LSN_h^g(s, q)$.*

Given a graph $G = (V, E)$ and a neighborhood subgraph ex-

Algorithm 2: TRAIN-DPGNN (Neighborhood Subgraph-based DPGNN)

Data: Graph $G = (V, E)$; Node features matrix $\mathbf{X}$; Maximum node degree θ; Negative sampling rate λ; Neighborhood radius h; Neighborhood subgraph extraction function g_n; Maximum # of iterations T.
Result: The trained model $\mathbf{\Theta}_T$.

Construct the set of training subgraphs and labels: $\mathcal{S} \leftarrow$ EXTRACT-SUBGRAPHS$(G, \theta, \lambda, h, g_n)$.
Compute σ via sensitivity analysis.
Initialize $\mathbf{\Theta}_0$ randomly.
for $t = 0$ *to* T **do**
  Sample set $\mathcal{B}_t \subseteq \mathcal{S}$ of size m uniformly.
  for *each* (S_{uv}, y_{uv}) *in* $\mathcal{B}_t$ **do**
    Compute gradient:
    $\mathbf{g}_t(S_{uv}, y_{uv}) \leftarrow \nabla_{\mathbf{\Theta}} \ell\left(R\left(\text{GNN}\left(\mathbf{A}_{uv}, \mathbf{X}_{uv}, \mathbf{\Theta}_t\right)\right), y_{uv}\right)$.
    Clip gradient:
    $\hat{\mathbf{g}}_t(S_{uv}, y_{uv}) \leftarrow \mathbf{g}_t(S_{uv}, y_{uv}) / \max\left(1, \frac{\|\mathbf{g}_t(S_{uv}, y_{uv})\|_2}{C}\right)$.
  $\overline{\mathbf{g}}_t \leftarrow \sum_{S_{uv}, y_{uv} \in \mathcal{B}_t} \hat{\mathbf{g}}_t(S_{uv}, y_{uv})$.
  Add noise: $\tilde{\mathbf{g}}_t \leftarrow \overline{\mathbf{g}}_t + \mathcal{N}\left(0, \sigma^2 \mathbb{I}\right)$.
  Update the parameters with rate η: $\mathbf{\Theta}_{t+1} \leftarrow \mathbf{\Theta}_t - \frac{\eta}{m} \overline{\mathbf{g}}_t$.

traction function g_n, the maximum of link dependency can be measured by the maximum of subgraph contextual neighbors of any link $(s, q) \in E$, i.e., $\max_{(s,q)\in E} |LSN_h^{g_n}(s, q)|$, which in turn determines the sensitivity. The following Lemma 1 shows the derivation of $LSN_h^{g_n}(s, q)$, and then Lemma 2 provides the upper bound of its maximum. Based on the derived bound, the sensitivity is given by Lemma 3.

Lemma 1. *Let (s, q) is any link in an undirected graph G, consider the following link sets after the graph projection and negative sampling:*

- $e_1 = \{(u, v) \mid u \in \Gamma_h(s) \cap \Gamma_h(q), v \in N_1(u) \cup \bar{N}_1(u)\}$;
- $e_2 = \{(u, v) \mid u \in \Gamma_h(s) \backslash \Gamma_h(q), v \in \Gamma_h(q) \backslash \Gamma_h(s)\}$.

then $LSN_h^{g_n}(s, q) = e_1 \cup e_2$.

Proof. Please refer to the full version [31]. □

Lemma 2. *Given an undirected graph $G = (V, E)$, let λ be the negative sampling rate for each node, $\theta > 2$ be the maximum node degree, and $h \geq 1$ be the radius of the neighborhood. Then, $\max_{(s,q)\in E} |LSN_h^{g_n}(s, q)|$ is upper bounded by $M_{g_n}(h, \theta, \lambda)$, where*

$$M_{g_n}(h, \theta, \lambda) = (1 + \lambda)\left(\theta^{h+1} + \sum\nolimits_{i=0}^{h-1} 2\theta^{i+1}\right) \quad (4)$$

Proof. Please refer to the full version [31]. □

Lemma 3 (Link-level Sensitivity of Neighborhood Subgraph-based GNN)**.** *Let G^θ be a graph with bounded degree θ, λ be the negative sampling rate, h be the radius of the neighborhood. Considering the batched gradient $\overline{\mathbf{g}}_t$ obtained from aggregating the gradient clipped by parameter C at step t in Algorithm 2. Let $M_{g_n}(h, \theta, \lambda)$ be the upper bound of dependency level derived in Lemma 2. Then the following inequality holds:*

$$\Delta(\overline{\mathbf{g}}_t) < 2C \cdot M_{g_n}(h, \theta, \lambda). \quad (5)$$

Proof. Please refer to the full version [31]. □

V. DPLP with Path Subgraph Extraction

The sensitivity analysis in Section IV reveals that, the number of subgraph contextual neighbors relies on the subgraph extraction procedure. While the h-hop neighborhood subgraph is effective at learning diverse heuristic methods for link prediction [6], the maximum of subgraph contextual neighbors is large even when $h = 1$, leading to a significant noise sensitivity. This motivates the design of a method that decreases the number of subgraph contextual neighbors while preserving the capability to efficiently learn informative heuristics. In this section, we present a balanced approach to subgraph extraction.

A. Path Subgraph

To reduce the noise sensitivity, in this section we propose an optimized path subgraph extraction approach, which exclusively extracts the links on paths between a pair of nodes. Formally, a k-hop path subgraph is defined as follows:

Definition 6 (K-Hop Path Subgraph)**.** *Given an undirected graph $G = (V, E)$ and a pair of distinct nodes $u, v \in V$, let P_{uv}^j be the set of paths from u to v with length j. For any link (u, v), the k-hop path subgraph S_{uv} consists of all the links $E_{uv} = \bigcup_{j=2}^{k} \bigcup_{w \in P_{uv}^j} \bigcup_{i=0}^{j-1} \{(w_i, w_{i+1})\}$.*

Figure 3 illustrates a comparison of neighborhood and path subgraphs. Figure 3(a) showcases the neighborhood subgraph for the link (u, v) when $h = 1$, which corresponds to a path subgraph with $k \leq 3$ in Figure 3(b). In the path subgraph, only the paths between (u, v) in the neighborhood are included, while redundant links (marked by blue links) and dangling links (marked by green links) are removed. Redundant links, which are induced by neighborhood nodes, fall out of any path from u to v with a length up to k. Dangling links connect dangling nodes, which are nodes that can only reach one of the vertices (u, v) within a 1-hop distance.

By excluding dangling links in the subgraph of a link, the path subgraph effectively reduces the number of subgraph contextual neighbors. The examples provided in Figure 4 clearly demonstrate our rationale for this approach.

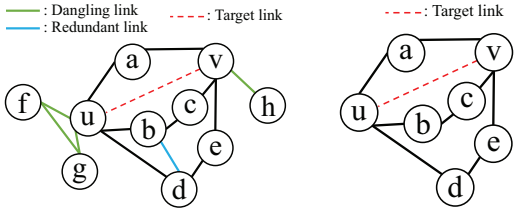

(a) 1-hop neighborhood subgraph (b) 3-hop path subgraph

Fig. 3: Examples of neighborhood and path subgraphs

Let's consider the impact of adding a link (u, g) to the graphs in Figure 4, where the maximum node degree $\theta = 5$. The link-based subgraph contextual neighbors of the link (u, g) in each subfigure are highlighted in red (excluding (u, g) itself). The red solid lines represent observed links, a.k.a. positive links, while the red dashed lines indicate negative links after negative sampling with a rate of λ. Figure 4(a) shows the case of extracting neighborhood subgraphs, while Figure 4(b) demonstrates the case of extracting path subgraphs.

Given the neighborhood radius $h = 1$, the neighborhood and path subgraph extraction functions are denoted as g_n and g_p, respectively. As shown in Figure 4(a), $\{(a, u), (b, u), (d, u), (f, u), (f, g)\} \subset LSN_1^{g_n}(u, g)$. And $\lambda\theta$ negative links incident to u, e.g., (u, v), are also encompassed within $LSN_1^{g_n}(u, g)$. This is because all these links fall into the set e_1 with $h = 1$ defined in Lemma 1, where $u \in N_0(u) \cap N_1(g)$ and $g \in N_0(g) \cap N_1(u)$. By comparison, as shown in Figure 4(b), when extracting the path subgraph from the same graph, $LSN_3^{g_p}(u, g) = \{(f, u), (f, g)\}$. This is because (u, g) is only on the paths from node f to g and u.

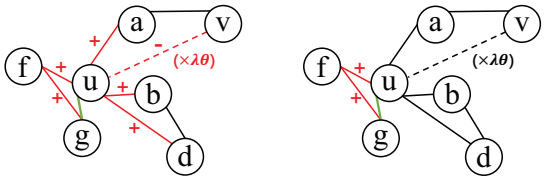

(a) Extracting Neighborhood Subgraphs (b) Extracting Path Subgraphs

Fig. 4: Link-based subgraph contextual neighbors of link (u, g) in neighborhood and path subgraphs, when $h = 1$

The following theorem establishes the theoretical analysis on data dependency of the proposed path-based subgraph extraction approach.

Theorem 1. *Given an undirected graph $G = (V, E)$, let λ be the negative sampling rate for each node and θ be the maximum node degree. For any $k, \theta \geq 2$, $\max_{(s,q)\in E} |LSN_k^{g_p}(s, q)|$ is bounded by $M_{g_p}(k, \theta, \lambda)$, where*

$$M_{g_p}(k, \theta, \lambda) = \sum_{i=0}^{h-1-r} 2\lambda\theta^{i+1} + 2\sum_{i=1}^{h-r} \min\{\theta^{h+1}, \theta^i\} + (1 + r)\theta^{h-r} \cdot \min\{(1 + \lambda)\theta, \theta^h\}, \tag{6}$$

and $h = \lfloor (k + 1)/2 \rfloor, r = (k - 1) \bmod 2$. Particularly, when $k = 2$, $M_{g_p}(k, \theta, \lambda) = 2\theta$.

Proof. Please refer to the full version [31]. □

Building on Lemma 2 and Theorem 1, the upper bound of the maximum number of contextual neighbors in a path subgraph can be reduced by at most θ^h, compared to an h-hop neighborhood subgraph.

B. Parameter selection

In this section, we design an indicator to better determine the parameters k and θ by considering the loss introduced by projection and gradient perturbation. Let $c \in \mathbb{R}^n$ be the degree distribution of a graph G, where n is the number of unique degrees, and each c_i denotes the number of nodes with degree i. Since c is computed on G, it should be perturbed by DP as well. Let c, c' denote the degree distribution computed on the neighboring graphs $G \simeq G'$ that differ in one link, the sensitivity can be bounded by

$$\|c - c'\|_2 \leq \sqrt{2}. \tag{7}$$

The private version of c is obtained by adding Gaussian noise as follows:

$$\tilde{c} = c + \mathcal{N}(0, \sigma^2 \mathbb{I}). \tag{8}$$

The loss caused by projection can be approximated as

$$\ell_{proj}(\theta, \tilde{c}) = \sum_{i=d^*}^{n} \tilde{c}_i \tag{9}$$

where $d^* = \min\{i \mid i > \theta, i \in \{1, 2, \cdots, n\}\}$. Given any k and θ, we design an indicator as $\frac{1}{\ell(k,\theta)}$, where $\ell(k, \theta)$ captures the projection and perturbation loss, which is defined as

$$\ell(k, \theta) = \frac{a|E|}{(1 - \gamma^k)(|E| - \ell_{proj})} + b \cdot \sigma_c(M, |E|, m, \varepsilon) \tag{10}$$

Note that in Equation 10, $|E|$ is the number of observed links in the original graph, and σ_c computes the noise multiplier with a given privacy budget ε, where $M = M_{g_p}(k, \theta, \lambda)$ in Equation 6, and m is the batch size. The first term computes the ratio of the total links to the remaining links after projection with a decaying factor $\gamma \in (0, 1)$ weighting the length of the path. The second terms approximates the magnitude of perturbation during DPGNN training. Two parameters a and b weight these two parts. Using this indicator, we can more adeptly choose optimal values for k and θ to minimize the overall loss introduced by the projection and perturbation process. The efficacy of this indicator will be further evaluated in Section VII.

VI. Theoretic Analyses

In this section, we establish theoretical analysis of the DPLP framework in terms of privacy and utility guarantee.

A. Privacy Analysis

The following theorem shows that DPLP achieves Link DP by offering $(\alpha, \varepsilon^\rho(\alpha))$-Rényi differential privacy. Here, according to [32], we use the functional view of Rényi differential privacy in which ε is a function of α, where $1 < \alpha < \infty$, and this function is determined by the private algorithm.

Theorem 2. *Let N be the number of training subgraphs, m be the batch size, g be the subgraph extraction function, h be the size of subgraphs, λ be the negative sampling rate, and θ be the maximum node degree, $M_g(h, \theta, \lambda)$ be the upper bound*

of subgraph contextual neighbors. Then, every iteration t of Algorithm 2 satisfies $(\alpha, \varepsilon^{\rho}(\alpha))$-Rényi DP, where

$$\varepsilon^{\rho}(\alpha) \leq \frac{1}{\alpha-1}\log\Bigg(1+\rho^2\binom{\alpha}{2}\min\Big\{4\left(e^{\varepsilon(2)}-1\right), e^{\varepsilon(2)}\min\Big\{2,\left(e^{\varepsilon(\infty)}-1\right)^2\Big\}\Big\} + \sum_{j=3}^{\alpha}\rho^j\binom{\alpha}{j}e^{(j-1)\varepsilon(j)}\min\Big\{2,\left(e^{\varepsilon(\infty)}-1\right)^j\Big\}\Bigg), \tag{11}$$

and

$$\rho = 1-\binom{N-M_g(h,\theta,\lambda)}{m}\Big/\binom{N}{m}. \tag{12}$$

By the standard composition theorem of Rényi Differential Privacy [33], over T iterations, Algorithm 2 is $(\alpha, \varepsilon^{\rho}(\alpha)T)$-Rényi DP.

Proof. Please refer to the full version [31]. □

Notably, the key difference of Theorem 2 from the unamplified Rényi differential privacy [33] is the introduction of ρ (as shown in Equation 12) to calculate the final privacy parameter. Given a graph, a smaller bound of dependency level $M_g(h,\theta,\lambda)$ leads to a smaller ρ, indicating a lower probability of including dependent subgraphs within each training batch. This reduction in ρ can enhance the effect of privacy amplification. Finally, we apply the conversion rule in [33] to convert the Rényi differential privacy back to the standard link DP.

B. Utility Analysis

Theorem 1 proves the advantage of the path subgraph compared to the neighborhood subgraph in terms of noise sensitivity. This improvement is primarily attributed to the fact that, when extracting the neighborhood subgraphs, many dangling links are included in sensitivity analysis as worst-case scenarios, leading to an increasing number of dependent links. By limiting the count of dangling edges, the sensitivity can be notably reduced.

Although the path subgraph effectively reduces the number of subgraph contextual neighbors, it unavoidably results in information loss when edges are dropped. One type of information missing in the path subgraph is the real node degrees. Degree information is widely utilized in local heuristic methods, especially those that rely on popularity measures (e.g., Preferential Attachment [34]). Nevertheless, there are global heuristic methods can be learned from path subgraphs [6]. The gloabl heuristic methods such as Common Neighbors, Local Path Index and Katz Index rely on predicting based on paths between nodes (u, v). The path subgraph-based DPLP makes the private learning of global heuristics achievable. Let S_{uv} denote the subgraph extracted by function g_p, we can establish the following Theorem.

Theorem 3. *Given a graph $G = (V, E)$ with maximum node degree D, let G^{θ} be the θ-bounded graph after projection with a threshold $\theta \leq D$. Let N be the number of training subgraphs, and M_{g_p} be the upper bound of the maximum number of path subgraph contextual neighbors in G. When $\theta \to D, (M_{g_p}-1)/N \to 0$, global heuristic score for (u, v) can be accurately approximated from the k-hop path subgraph S_{uv} around (u, v) and the approximation error decreases at least exponentially with k.*

Proof. Please refer to the full version [31]. □

Theorem 3 not only establishes that the global heuristics can be estimated by the path subgraph-based DPLP method, but also indicates that using smaller-scale local path subgraphs (i.e., smaller k) can lead to accurate approximations. This suggests the potential for precise learning of a wide range of higher-order path-based heuristics with minimal error from fewer-hop path subgraphs, and allows the proposed method to reach the expressive power of multi-layer GNNs with fewer layers.

C. Time Complexity Analysis

In order to present the performance of the DPLP methods, we analyze the time complexity of Algorithm 2. Let $d(v)$ be the degree of node v, and $d_{\max}$ be the max degree in the original graph, we analyze the time complexity in different phases of Algorithm 2 as follows.

Projection: In Algorithm 1, the function iterates through each node v in V, sampling up to θ immediate neighbors in $O(\theta)$ time and updating the filtered edge set E^{θ} can be completed in constant time through the adjacency matrix. Hence, the total loop's time complexity is $O(|V| \cdot \theta)$, combining initialization for overall complexity.

Subgraph extraction: According to the Algorithm 1, the subgraph extraction process iterates through all nodes v in V, uniformly sampling v's negative edges in $O(\lambda\theta)$ time and adding non-neighbors $\bar{N}_1(v)$ to the negative edge set *NE* instantly. For each v, it examines nodes in $N_1(v) \cup \bar{N}_1(v)$, employing function g to extract subgraph S_{vi} in $O(g(h))$ time. Specifically, for neighborhood subgraphs, Breadth-First Search (BFS) identifies h-hop neighbors within $O(\theta^h)$ time, while Depth-First Search (DFS) locates k-hop path subgraphs in $O(\theta^k)$ time. Assigning y_{vi} values, based on i's presence in $N_1(v)$, is immediate. Consequently, the complexity of the inner loop is $O((1+\lambda)\theta)$, resulting in an overall complexity for Algorithm 1 of $O(|V| \cdot \theta^{h+1})$. For path subgraph extraction, the time complexity is $O(|V| \cdot \theta^{k+1})$.

Training iterations: Assume the GNN model's complexity for processing a single instance is $O(f)$, where f is a function representing the computational cost of the GNN over the subgraph. Thus, the main training loop contributes $O(T \cdot m \cdot f)$, where T is the number of iterations, and m represents the times for gradient clipping within a batch.

Therefore, the overall time complexity of the Algorithm 2 can be approximated as $O(|V| \cdot \theta^{\xi+1}) + O(T \cdot m \cdot f)$, where ξ denotes either neighborhood radius h or the path length k, contingent upon the subgraph extraction function utilized. When we apply the path subgraph-based method to extremely large and dense graphs and explore paths with a large length k,

the cost of extracting subgraphs $O(|V| \cdot \theta^{k+1})$ is the dominant term. Nevertheless, in most real-world graph data scenarios, as demonstrated by Theorem 3, employing path subgraphs with a small k suffices for the majority of cases. Moreover, because the extraction of subgraphs is independent, it allows for parallelization and ensures algorithm's practical efficiency. We validate these analytical results in Section VII-B.

VII. Experimental Evaluations

In this section, we conduct extensive experiments to empirically evaluate DPLP's performance in terms of privacy, accuracy, and the effectiveness of parameter selection.

A. Experimental Setting

Dataset. We evaluate the proposed methods on several publicly available link prediction datasets, by considering varying degree distributions, and the numbers of nodes and edges.

- USAir [1] is a network of US Airlines with 332 nodes and 2,126 edges. The average node degree is 12.81.
- PB [2] is a network of US political blogs with 1,222 nodes and 16,714 edges. The average node degree is 27.36.
- Yeast [3] is a protein-protein interaction network in yeast with 2,375 nodes and 11,693 edges. The average node degree is 9.85.
- C.ele [4] is a neural network of C. elegans with 297 nodes and 2,148 edges. The average node degree is 14.46.

Experiment Design. We implement DPLP with neighborhood subgraph extraction as our baseline, referred to as DPLP-NS. Next, we optimize the subgraph extraction module of DPLP by implementing path subgraph extraction, denoted as DPLP-PS. We then compare our methods with three other techniques: SEAL [6], which represents a non-private GNN method for link prediction, LapGraph [9], which is a state-of-the-art differentially private technique designed for graph data, and FKGE, which learns differentially private graph embedding for link prediction. [29] The aggregation perturbation method [10] and other gradient perturbation method [13] are not suitable for comparison in our experiments, as these methods are exclusively applicable to node-level tasks.

Implementation and Parameters. For DPLP methods (DPLP-NS and DPLP-PS), we use GCN as the default architecture of SGNN, and we set the number of SGNN layers to k for DPLP-PS and $h = \lfloor (k+1)/2 \rfloor$ for DPLP-NS. For the LapGraph method, we use the SGNN based on the neighborhood subgraph as its backbone for link prediction. Similar to DPLP-NS, the number of layers is set to $h = \lfloor (k+1)/2 \rfloor$. For all subgraph-based methods, we use the Double-Radius Node Labeling (DRNL) as the labeling method [6]. We set the number of hidden units to 32, and use the Relu activation function at every layer. Dropout layers are also used for all methods.

[1] http://vlado.fmf.uni-lj.si/pub/networks/data/mix/USAir97.net
[2] https://sites.cc.gatech.edu/dimacs10/archive/clustering.shtml
[3] http://vlado.fmf.uni-lj.si/pub/networks/data/bio/Yeast/Yeast.htm
[4] https://snap.stanford.edu/data/C-elegans-frontal.html

We train all methods over 50 epochs with a batch size of 1024 on PB, and 128 on the rest 3 datasets, i.e., USAir, Yeast and Celegans. For DPLP-NS, DPLP-PS, we use the same parameter setting for training GNN modules. We train all the methods with a learning rate of 0.01 and repeat each combination of possible hyperparameter values 10 times. Since the original FKGE algorithm is primarily designed for knowledge graph, to accommodate the datasets used in this experiment, we learn the graph embedding from scratch. For fairness, similarly to other methods, FKGE is applied in a centralized setting. Specifically, after obtaining the embeddings, FKGE trains the differentiall private version of these embeddings via PATE-GAN [29] locally. Aligned with the original works, the number of teachers is set to 32.

Performance Measurement. Area Under the Curve (AUC) is a commonly used performance measurement of a binary classification model [35]. AUC ranges from 0 to 1, with a higher value indicating better model performance. In the experiment, we pick the best-performing model based on validation AUC and report the average test AUC with standard error.

Privacy setting. We numerically calibrate the noise scale (i.e., the noise standard deviation σ divided by the sensitivity) of the DPLP-NS and DPLP-PS methods and the Gaussian mechanism to achieve the desired (ε, δ)-Link DP with 0.1ε for parameter selection. We report results for several values of ε, while δ is set to be smaller than the inverse number of private entities (i.e., links for link-level privacy).

All the models are implemented in PyTorch using PyTorch-Geometric (PyG). Experiments are conducted on two devices with NVIDIA GeForce RTX 4090 GPUs, Intel Xeon 6238 CPUs, and 32 GB RAM.

B. Experimental Results and Analysis

1) Overall Results: We first compare the AUC of our proposed methods against the non-private and the differentially private baseline (i.e., LapGraph and FKGE). We fix the privacy budget to $\varepsilon = 4$ for the private methods. The results are presented in Table II. We observe that the proposed path subgraph-based method (DPLP-PS) is competitive with SEAL, with a decrease within 6.5% in AUC on the four datasets. DPLP-PS significantly outperforms the private competitors LapGraph, FKGE and DPLP-NS. The AUC of DPLP-PS surpasses that of LapGraph by approximately 37, 16, 25, and 5 points for the Yeast, USAir, C.ele, and PB datasets, respectively. Furthermore, it exhibits an increase of roughly 5, 7, 6, and 4 points compared to FKGE across the same datasets.

The DPLP-NS model performs better than LapGraph on the Yeast, USAir, and C.ele datasets, demonstrating the argument that our gradient-perturbation paradigms are superior to input perturbation methods under strict privacy requirement. However, on the PB dataset, LapGraph achieves a higher AUC by approximately 4 points compared to DPLP-NS. This discrepancy can be attributed to the high average degree in PB, necessitating a higher θ to retain sufficient training samples. Nevertheless, an excessively large θ in DPLP-NS results in

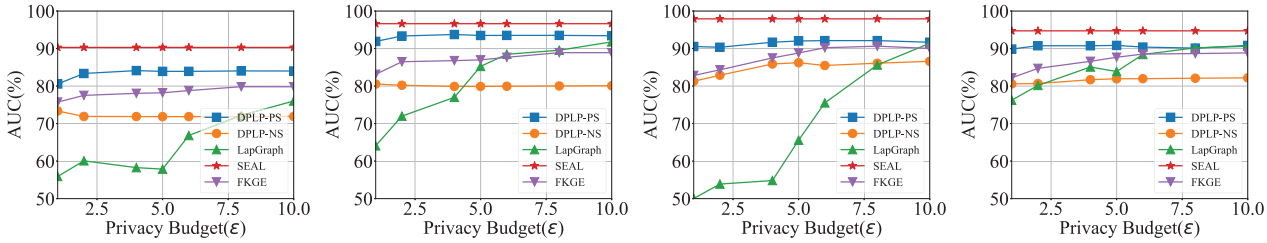

(a) C.ele (b) USAir (c) Yeast (d) PB

Fig. 5: Results of AUC by varying privacy budgets.

TABLE II: **Test AUC(%) of different methods with $\varepsilon = 4$. The best-performing private method is highlighted.**

Model	Yeast	USAir	C.ele	PB
SEAL	97.91 ± 0.52	96.62 ± 0.72	90.30 ± 1.35	94.72 ± 0.46
LapGraph	54.82 ± 8.90	76.99 ± 11.18	58.26 ± 15.25	85.08 ± 5.24
FKGE	87.49 ± 2.24	86.78 ± 3.23	78.07 ± 1.49	86.59 ± 0.37
DPLP-NS	85.89 ± 7.26	79.90 ± 14.09	71.88 ± 5.94	81.69 ± 11.66
DPLP-PS	$\mathbf{92.02 \pm 1.18}$	$\mathbf{93.74 \pm 0.04}$	$\mathbf{84.12 \pm 0.29}$	$\mathbf{90.75 \pm 0.24}$

high sensitivity, thereby impacting the model's performance-a phenomenon not significantly observed in DPLP-PS. This results substantiates our theoretical findings that DPLP-PS enhances the model performance of privacy models on dense datasets by learning with lower sensitivity.

According to Table II, we observe that FKGE consistently outperforms DPLP-NS across all datasets. This indicates that at high dependency levels, the noise introduced by DP diminishes the expressive power of GNNs, rendering them less effective compared to FKGE. Conversely, DPLP-PS surpasses FKGE in all datasets, highlighting the efficiency of path subgraph extraction in reducing dependency levels and improving privacy amplification.

As shown in Figure 5, as ε increases, the suboptimal outcomes following FKGE's convergence reveal its limitations in link prediction. This is primarily due to FKGE's use of translation or latent factor models for graph embeddings, which struggle to capture structural node similarities [36]. Additionally, the graph embeddings might necessitate large dimensions to express some simple heuristics, leading to inferior performance under DP noise compared to global heuristics [37]. In contrast, DPLP-PS employs GNN models capable of learning structural similarities between nodes based on path subgraphs. Its superior performance over FKGE across all privacy budgets validates Theorem 3, demonstrating that DPLP-PS can maintain link prediction accuracy by learning various global heuristics.

To study the impact of different privacy budgets on the performance of link prediction, we present the AUC for each method by varying ε from 1 to 10. The results are illustrated in Figure 5. It's obvious that DPLP-PS consistently outperforms LapGraph, FKGE and DPLP-NS, particularly in more strict privacy settings (i.e., when given a small privacy budget). Specifically, DPLP-NS converges to its optimal value faster, yielding a superior AUC than LapGraph when the privacy budget is stringent (i.e., $\varepsilon \leq 2.5$). However, due to the larger noise added by DPLP-NS, it has a larger standard deviation, making its performance less stable. As the privacy budget increases, it is eventually surpassed by LapGraph.

The performance gap between DPLP methods and LapGraph is influenced by the dataset's degree distribution. For instance, on the Yeast dataset, which has lowest average degree, LapGraph necessitates a high privacy budget (with $\varepsilon > 7.5$) to achieve satisfactory accuracy. Conversely, on PB, possessing the highest average degree, LapGraph surpasses the DPLP-NS baseline with a privacy budget of merely 2.5. Notably, the AUC of DPLP-PS method that of the non-private SEAL with much smaller privacy budgets and consistently outperforms LapGraph when $\varepsilon < 10$. This notable performance gap is attributed to LapGraph's direct perturbation of input, which alters the sparsity of the original graph. The sparsity of the graph serves as a crucial feature influencing the performance of link prediction models. Experimental results validate this observation, as LapGraph performs most poorly on the most sparse Yeast dataset, with a AUC gap of over 30% compared to DPLP-PS when $\varepsilon < 2.5$.

2) Correctness of the indicator design: We now validate the correctness of our designed performance indicator (see Equation 10) by comparing its values i.e., $\frac{1}{\ell(k,\theta)}$, with the performance of DPLP. By varying combinations of (θ, k), we report the values of indicator and the AUC of DPLP-PS on four datasets in Figure 6, where the privacy budget $\varepsilon = 11$ (with 0.1ε for computing indicator). We can observe that, the AUC and the indicator values show a similar trend across different combinations of (θ, k) on all datasets. This indicates that our designed loss function accurately captures the projection and perturbation loss, enabling DPLP-PS to benefit from parameter selection effectively.

On the USAir and PB datasets, fluctuations in data points are observed, and the prediction of trends for specific points deviates, such as the transition from point $(60, 3)$ to $(60, 4)$ on USAir. This is attributed to the relatively small size of these datasets, introducing biases in estimating projection and perturbation losses. However, even with such challenges, DPLP-PS remains viable to avoid unfavorable parameter selections on both datasets. This demonstrates the capability of our designed loss function to serve as a performance indicator and save privacy budget for expensive hyperparameter searching.

3) Ablation study on parameters k and θ: Now we further study the impact of parameters k and θ on the performance of DPLP-PS, respectively. As for the number of hops k, we restrict our selection of k to the set $\{2, 3, 4\}$. This decision is informed by two primary observations. Firstly, empirical

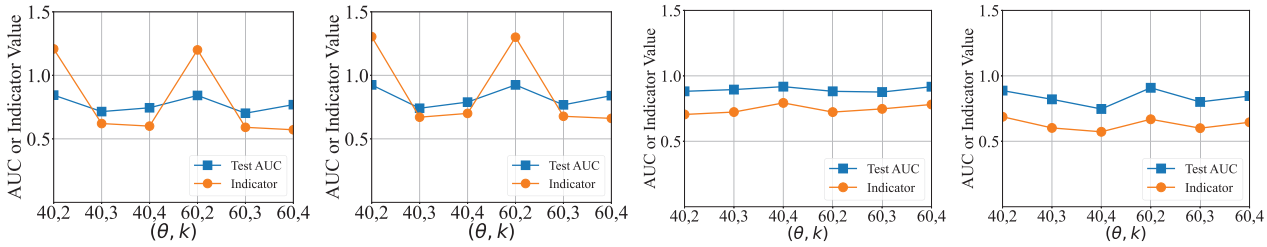

(a) C.ele (b) USAir (c) Yeast (d) PB

Fig. 6: Comparison of indicator value and AUC of DPLP-PS.

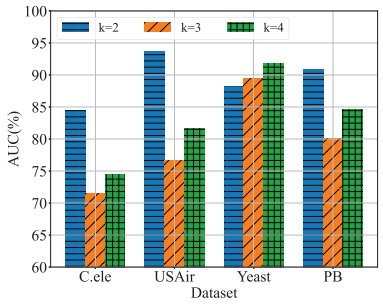

Fig. 7: Effect of the number of hops k on the AUC performance of the DPLP-PS on 4 datasets.

assessments reveal that performance generally plateaus or does not improve significantly for $k \geq 5$ [6]. This aligns with our theoretical findings emphasizing that the most valuable information predominantly resides within shorter paths. Secondly, even at $k = 4$, the inclusion of a hub node can sometimes lead to exceedingly large subgraphs. Based on this setting, we report the AUC under a privacy budget of $\varepsilon = 4$. The findings are presented in Figure 7.

We observe that DPLP-PS exhibited peak performance for $k = 2$ on the C.ele, USAir, and PB datasets. For these datasets, as k increases to 4, the AUC of the DPLP-PS initially declines at $k = 3$ and then rebounds at $k = 4$. This fluctuation can be attributed to the fact that involving more hops augments the noise in the gradient, which in turn negatively impacts the model's AUC. Yet, with an increased k, the model can leverage information from more distant nodes for predictions, potentially counterbalancing the gradient perturbation. This phenomenon is particularly pronounced in datasets with a smaller average degree. As illustrated in Figure 7, DPLP-PS optimally capitalizes on multiple hops within the Yeast dataset, achieving the highest efficacy at $k = 4$. This is because the information aggregated from more distant nodes is sufficient to compensate for the introduced noise from a larger k.

Then we study the influence of threshold θ on the AUC of DPLP-PS, where θ varies from 20 to 100 and the privacy budget ε is set to 3 or 11. Figure 8 shows that the AUC keeps growing with θ on PB (which has a high average degree), while on C.ele, USAir and Yeast (with lower average degrees), the AUC increases with θ up to a peak point around 40 or 60, and then becomes steady or decreases. This is due to the trade-off between having more samples for training and the amount of noise injected: the larger θ, the fewer samples are excluded from the aggregations (i.e., less information loss), but on the other hand, a larger sensitivity of the batched gradient introduces more noise.

4) Results with different GNN architectures and link prediction strategies: As mentioned in Section IV, the proposed DPLP paradigm can be implemented with most GNN architectures. We investigate the performance of DPLP-PS with three more GNN architectures apart from the default GCN architecture, namely GraphSAGE [38], GIN [39] and DGCNN [40]. The results are shown in the Table III.

We observed that GraphSAGE exhibits the least effective performance. This can be attributed to its method of employing the Hadamard product for pairwise node representations derived from a GNN, while omitting the use of a labeling trick [6]. Consequently, it fails to learn even basic neighborhood-overlap heuristics, confirming our arguments in the Introduction. Furthermore, our analysis shows a marginally better performance of GIN compared to GCN. This improvement stems from GIN's substitution of linear feature transformations in GCN with Multi-Layer Perceptrons (MLPs), enhancing its expressiveness in message-passing-based GNNs. As for DGCNN, it features a SortPooling readout layer that comprehensively processes all nodes in the enclosing subgraph. This methodology markedly improves its performance in specific datasets, notably Yeast, C.ele, and PB. However, there is a minor decline in effectiveness when applied to the USAir dataset. This variation in performance underlines the fact that employing a subgraph readout layer can be beneficial in certain contexts, a point that resonates with our initial discussion in the Introduction.

The aforementioned findings illustrate that DPLP is adaptable across a range of GNN architectures. Notably, even the GAE, which shows the least performance, can yield a model of acceptable usability. Despite the potential superiority of other models on varied datasets, GCN remains the preferred framework for DPLP. This preference is due to GCN's extensive application and its ability to outperform other architectures in certain scenarios, such as with the USAir dataset.

We then apply DPLP to the state-of-the-art model ELPH for link prediction [17] to demonstrate that the proposed framework can be implemented with more advanced algorithms other than SEAL. Although subgraphs are not explicitly

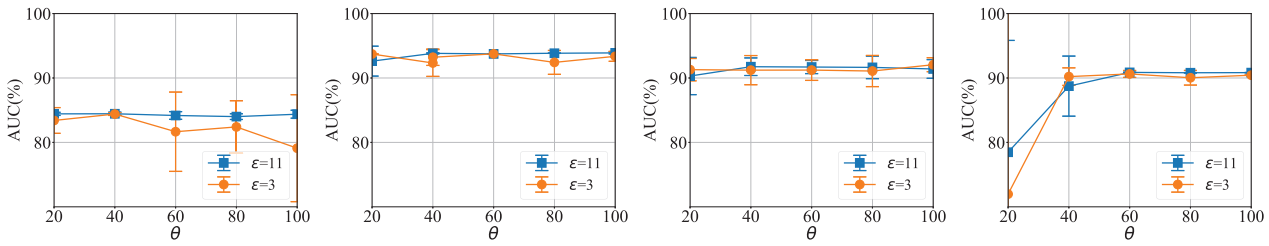

(a) C.ele (b) USAir (c) Yeast (d) PB

Fig. 8: Impact of the threshold θ on the AUC performance of DPLP-PS.

TABLE III: **Test AUC(%) of different GNN architectures with $\varepsilon = 4$. The best result on each dataset is highlighted.**

Model	Yeast	USAir	C.ele	PB
GCN	92.02 ± 1.18	$\mathbf{93.74 \pm 0.04}$	84.12 ± 0.29	90.75 ± 0.24
GraphSAGE	84.23 ± 1.25	86.29 ± 0.79	77.34 ± 2.37	80.53 ± 0.74
GIN	93.23 ± 1.24	93.48 ± 0.96	85.73 ± 0.18	91.79 ± 0.09
DGCNN	$\mathbf{94.76 \pm 0.96}$	93.33 ± 0.47	$\mathbf{88.75 \pm 0.54}$	$\mathbf{92.87 \pm 0.08}$

extracted in ELPH, this method estimates the structure features within neighborhood subgraphs for link embedding learning. Thus, the sensitivity can be computed by our analytical results, and our gradient perturbation method can be applied to ensure DP training. Comparative results are shown in the Table IV. Although ELPH outperforms SEAL, its dependency level remains high as it is still based on neighborhood subgraphs, resulting its private method (i.e., DPLP-ELPH) in greater magnitude of noises and loss of utility. This demonstrates that even the best methods in non-private settings need to be re-evaluated for their utility under DP.

TABLE IV: **Test AUC(%) of different link prediction model with $\varepsilon = 1, 10$. The best result on each dataset is highlighted.**

Model	Privacy level	Yeast	USAir	C.ele	PB
SEAL	N/A	92.02 ± 1.18	93.74 ± 0.04	84.12 ± 0.29	90.75 ± 0.24
ELPH	N/A	94.13 ± 1.02	95.82 ± 0.02	86.23 ± 0.18	93.25 ± 0.16
DPLP-PS	$\varepsilon = 1$	90.54 ± 3.39	91.90 ± 3.49	80.56 ± 7.53	89.87 ± 8.35
	$\varepsilon = 10$	91.68 ± 1.39	93.42 ± 0.85	84.01 ± 0.21	90.83 ± 0.55
DPLP-ELPH	$\varepsilon = 1$	83.28 ± 5.26	82.54 ± 12.23	75.37 ± 4.07	82.59 ± 10.06
	$\varepsilon = 10$	86.60 ± 3.19	82.09 ± 11.93	77.90 ± 2.78	84.18 ± 8.62

5) Time consumption: We evaluate the time cost of DPLP methods in different phases and compare them with that of the ground truth (i.e., SEAL). We extract subgraphs using 8 parallel processors. As indicated in Table V, DPLP-PS exhibits a higher time cost for subgraph extraction compared to other methods, consistent with the time complexity analysis in Section VI-B. DPLP-PS requires additional time to identify the path between target node pairs compared to DPLP-NS, particularly evident in the Yeast and PB datasets, indicating an increase in time cost with graph size expansion. This discrepancy is attributed to the maximum path length k of 4 in the Yeast dataset. Notably, DPLP-PS features slightly lower training time than DPLP-NS due to the smaller size of the path subgraph, reducing computational workload. Conversely, DPLP-NS exhibits higher subgraph extraction time than SEAL due to projection operations, albeit the difference is marginal since both methods extract neighborhood subgraphs. Additionally, the training time of DPLP-NS surpasses that of SEAL slightly, attributable to the gradient clipping required within batches during DPLP's training process. Furthermore, we can use more processors to improve the efficiency, the results are shown in [31]

TABLE V: **The time costs (s) of SEAL, DPLP-NS and DPLP-PS in different phases.**

Method	Phase	Yeast	USAir	C.ele	PB
SEAL	Subgraph Extraction	3.52	0.48	0.52	2.54
	Training(per epoch)	0.08	0.08	0.07	0.12
DPLP-NS	Subgraph Extraction	3.67	0.50	0.52	3.00
	Training(per epoch)	0.51	0.22	0.18	0.24
DPLP-PS	Subgraph Extraction	150.02	2.15	2.53	80.00
	Training(per epoch)	0.22	0.12	0.11	0.2

VIII. Conclusion

This work introduces a pioneering privacy-preserving link prediction framework, named DPLP. DPLP is the first work to learn differentially private GNNs tailored to link prediction, while being adaptable across various GNN architectures. Within DPLP framework, the subgraph extraction module serves as the building block to achieve high model utility. A neighborhood subgraph extraction method is first designed for DPLP, then we optimize it by devising a path subgraph extraction scheme, which minimizes data dependency by concentrating on the information within the paths connecting the nodes of a target link. As a result, we have achieved notable improvements in prediction accuracy. Our extensive theoretical analysis, encompassing both privacy and utility dimensions, validates the framework's efficacy.

In future work, we aim to investigate whether the most appropriate subgraph construction method can be determined using our dataset knowledge. A key challenge involves devising a versatile sensitivity analysis method suitable for various subgraph construction techniques. Our future objectives include investigating the possible approaches such as local sensitivity to tackle the above challenges, and extend the framewrok to more strict privacy protection scenarios.

Acknowledgement

This work was supported by the National Natural Science Foundation of China (Grant No: 62102334, 92270123 and 62372122), and the Research Grants Council, Hong Kong SAR, China (Grant No: 12200021, 15210023 and C2004-21GF).

REFERENCES

[1] D. Liben-Nowell and J. Kleinberg, "The link-prediction problem for social networks. journal of the association for information science and technology (2007)," *Google Scholar Google Scholar Digital Library Digital Library*, 2007.

[2] L. A. Adamic and E. Adar, "Friends and neighbors on the web," *Social networks*, vol. 25, no. 3, pp. 211–230, 2003.

[3] J. Bennett, S. Lanning *et al.*, "The netflix prize," in *Proceedings of KDD cup and workshop*, vol. 2007. New York, 2007, p. 35.

[4] N. Shibata, Y. Kajikawa, and I. Sakata, "Link prediction in citation networks," *Journal of the American society for information science and technology*, vol. 63, no. 1, pp. 78–85, 2012.

[5] M. Zhang, P. Li, Y. Xia, K. Wang, and L. Jin, "Revisiting graph neural networks for link prediction," 2020.

[6] M. Zhang and Y. Chen, "Link prediction based on graph neural networks," *Advances in neural information processing systems*, vol. 31, 2018.

[7] M. Fredrikson, S. Jha, and T. Ristenpart, "Model inversion attacks that exploit confidence information and basic countermeasures," in *Proceedings of the 22nd ACM SIGSAC conference on computer and communications security*, 2015, pp. 1322–1333.

[8] R. Shokri, M. Stronati, C. Song, and V. Shmatikov, "Membership inference attacks against machine learning models," in *2017 IEEE symposium on security and privacy (SP)*. IEEE, 2017, pp. 3–18.

[9] F. Wu, Y. Long, C. Zhang, and B. Li, "Linkteller: Recovering private edges from graph neural networks via influence analysis," in *2022 IEEE Symposium on Security and Privacy (SP)*. IEEE, 2022, pp. 2005–2024.

[10] S. Sajadmanesh, A. S. Shamsabadi, A. Bellet, and D. Gatica-Perez, "Gap: Differentially private graph neural networks with aggregation perturbation," in *USENIX Security 2023-32nd USENIX Security Symposium*, 2023.

[11] S. Sajadmanesh and D. Gatica-Perez, "Locally private graph neural networks," in *Proceedings of the 2021 ACM SIGSAC conference on computer and communications security*, 2021, pp. 2130–2145.

[12] W. Lin, B. Li, and C. Wang, "Towards private learning on decentralized graphs with local differential privacy," *IEEE Transactions on Information Forensics and Security*, vol. 17, pp. 2936–2946, 2022.

[13] A. Daigavane, G. Madan, A. Sinha, A. G. Thakurta, G. Aggarwal, and P. Jain, "Node-level differentially private graph neural networks," *arXiv preprint arXiv:2111.15521*, 2021.

[14] B. Perozzi, R. Al-Rfou, and S. Skiena, "Deepwalk: Online learning of social representations," in *Proceedings of the 20th ACM SIGKDD international conference on Knowledge discovery and data mining*, 2014, pp. 701–710.

[15] A. Grover and J. Leskovec, "node2vec: Scalable feature learning for networks," in *Proceedings of the 22nd ACM SIGKDD international conference on Knowledge discovery and data mining*, 2016, pp. 855–864.

[16] P. Lops, M. De Gemmis, and G. Semeraro, "Content-based recommender systems: State of the art and trends," *Recommender systems handbook*, pp. 73–105, 2011.

[17] B. P. Chamberlain, S. Shirobokov, E. Rossi, F. Frasca, T. Markovich, N. Hammerla, M. M. Bronstein, and M. Hansmire, "Graph neural networks for link prediction with subgraph sketching," *ICLR*, 2023.

[18] Q. Ye, H. Hu, M. H. Au, X. Meng, and X. Xiao, "Lf-gdpr: A framework for estimating graph metrics with local differential privacy," *IEEE Transactions on Knowledge and Data Engineering*, vol. 34, no. 10, pp. 4905–4920, 2020.

[19] Y. Xiao, Q. Ye, H. Hu, H. Zheng, C. Fang, and J. Shi, "Mexmi: Pool-based active model extraction crossover membership inference," *Advances in Neural Information Processing Systems*, vol. 35, pp. 10 203–10 216, 2022.

[20] U. Weinsberg, S. Bhagat, S. Ioannidis, and N. Taft, "Blurme: Inferring and obfuscating user gender based on ratings," in *Proceedings of the sixth ACM conference on Recommender systems*, 2012, pp. 195–202.

[21] A. Narayanan and V. Shmatikov, "Robust de-anonymization of large sparse datasets," in *2008 IEEE Symposium on Security and Privacy (sp 2008)*. IEEE, 2008, pp. 111–125.

[22] A. Epasto, V. Mirrokni, B. Perozzi, A. Tsitsulin, and P. Zhong, "Differentially private graph learning via sensitivity-bounded personalized pagerank," *Advances in Neural Information Processing Systems*, vol. 35, pp. 22 617–22 627, 2022.

[23] J. A. Calandrino, A. Kilzer, A. Narayanan, E. W. Felten, and V. Shmatikov, ""you might also like:" privacy risks of collaborative filtering," in *2011 IEEE symposium on security and privacy*. IEEE, 2011, pp. 231–246.

[24] A. De and S. Chakrabarti, "Differentially private link prediction with protected connections," in *Proceedings of the AAAI conference on artificial intelligence*, vol. 35, no. 1, 2021, pp. 63–71.

[25] S. P. Liew, T. Takahashi, S. Takagi, F. Kato, Y. Cao, and M. Yoshikawa, "Network shuffling: Privacy amplification via random walks," in *Proceedings of the 2022 International Conference on Management of Data*, 2022, pp. 773–787.

[26] A. Friedman, S. Berkovsky, and M. A. Kaafar, "A differential privacy framework for matrix factorization recommender systems," *User Modeling and User-Adapted Interaction*, vol. 26, pp. 425–458, 2016.

[27] M. Abadi, A. Chu, I. Goodfellow, H. B. McMahan, I. Mironov, K. Talwar, and L. Zhang, "Deep Learning with Differential Privacy," *Proceedings of the 2016 ACM SIGSAC Conference on Computer and Communications Security*, pp. 308–318, Oct. 2016.

[28] T. T. Mueller, J. C. Paetzold, C. Prabhakar, D. Usynin, D. Rueckert, and G. Kaissis, "Differentially private graph classification with gnns," *arXiv preprint arXiv:2202.02575*, 2022.

[29] H. Peng, H. Li, Y. Song, V. Zheng, and J. Li, "Differentially private federated knowledge graphs embedding," in *Proceedings of the 30th ACM International Conference on Information & Knowledge Management*, 2021, pp. 1416–1425.

[30] H. Sun, X. Xiao, I. Khalil, Y. Yang, Z. Qin, H. Wang, and T. Yu, "Analyzing subgraph statistics from extended local views with decentralized differential privacy," in *Proceedings of the 2019 ACM SIGSAC Conference on Computer and Communications Security*, 2019, pp. 703–717.

[31] X. Ran, Q. Ye, H. Hu, X. Huang, J. Xu, and J. Fu, "Differentially private graph neural networks for link prediction," https://github.com/marlowe518/Awesome-Differential-Privacy-and-Meachine-Learning/tree/20230731/GNN/differentially_private_link_prediction, 2023.

[32] Y.-X. Wang, B. Balle, and S. P. Kasiviswanathan, "Subsampled rényi differential privacy and analytical moments accountant," in *The 22nd International Conference on Artificial Intelligence and Statistics*. PMLR, 2019, pp. 1226–1235.

[33] I. Mironov, "Rényi differential privacy," in *2017 IEEE 30th computer security foundations symposium (CSF)*. IEEE, 2017, pp. 263–275.

[34] A. Kumar, S. S. Singh, K. Singh, and B. Biswas, "Link prediction techniques, applications, and performance: A survey," *Physica A: Statistical Mechanics and its Applications*, vol. 553, p. 124289, 2020.

[35] A. P. Bradley, "The use of the area under the roc curve in the evaluation of machine learning algorithms," *Pattern recognition*, vol. 30, no. 7, pp. 1145–1159, 1997.

[36] L. F. Ribeiro, P. H. Saverese, and D. R. Figueiredo, "struc2vec: Learning node representations from structural identity," in *Proceedings of the 23rd ACM SIGKDD international conference on knowledge discovery and data mining*, 2017, pp. 385–394.

[37] L. Wu, P. Cui, J. Pei, L. Zhao, and X. Guo, "Graph neural networks: Foundation, frontiers and applications," in *Proceedings of the 28th ACM SIGKDD Conference on Knowledge Discovery and Data Mining*, 2022, pp. 4840–4841.

[38] W. L. Hamilton, "Graph representation learning," *Synthesis Lectures on Artifical Intelligence and Machine Learning*, vol. 14, no. 3, pp. 1–159, 2020.

[39] K. Xu, W. Hu, J. Leskovec, and S. Jegelka, "How powerful are graph neural networks?" *arXiv preprint arXiv:1810.00826*, 2018.

[40] M. Zhang, Z. Cui, M. Neumann, and Y. Chen, "An End-to-End Deep Learning Architecture for Graph Classification," *Proceedings of the AAAI Conference on Artificial Intelligence*, vol. 32, no. 1, Apr. 2018.